NANOSYSTEMS:
PHYSICS, CHEMISTRY, MATHEMATICS

Original article

Kolmanovich D.D., et al. *Nanosystems: Phys. Chem. Math.*, 2024, **15** (5), 675–682.
http://nanojournal.ifmo.ru
DOI 10.17586/2220-8054-2024-15-5-675-682

Proton beam-induced radiosensitizing effect of $Ce_{0.8}Gd_{0.2}O_{2-x}$ nanoparticles against melanoma cells *in vitro*

Danil D. Kolmanovich[1,a], Mikhail V. Romanov[2,3,b], Sergey A. Khaustov[4,c], Vladimir K. Ivanov[5,d], Alexander E. Shemyakov[1,6,e], Nikita N. Chukavin[1,4,f], Anton L. Popov[1,4,g]

[1]Institute of Theoretical and Experimental Biophysics of the Russian Academy of Sciences, Pushchino, Russia
[2]Institute of Molecular Theranostics, Sechenov First Moscow State Medical University, Moscow, Russia
[3]Lopukhin Federal Research and Clinical Center of Physical-Chemical Medicine of Federal Medical Biological Agency, Moscow, Russia
[4]Scientific and Educational Center, State University of Education, Moscow, Russia
[5]Kurnakov Institute of General and Inorganic Chemistry of the Russian Academy of Sciences, Moscow, Russi
[6]Lebedev Physical Institute of the Russian Academy of Sciences, Moscow, Russia

[a]kdd100996@mail.ru, [b]romanov.mikhail@phystech.edu, [c]sergeykhaustov@gmail.com, [d]van@igic.ras.ru, [e]alshemyakov@yandex.ru, [f]chukavinnik@gmail.com, [g]antonpopovleonid@gmail.com

Corresponding author: A. L. Popov, antonpopovleonid@gmail.com

ABSTRACT Proton beam therapy is being used increasingly to treat melanoma. Meanwhile, proton beam therapy has a number of disadvantages that can be reduced or completely eliminated through the use of modern innovative approaches, including the use of nanoradiosensitizers. Here we showed the possibility of using redox-active dextran-stabilized $Ce_{0,8}Gd_{0,2}O_{2-x}$ nanoparticles ($Ce_{0,8}Gd_{0,2}O_{2-x}$ NPs) as a radiosensitizer to promote mouse melanoma cell death under proton beam irradiation *in vitro*. It has been shown that these $Ce_{0,8}Gd_{0,2}O_{2-x}$ NPs do not reduce the viability and survival rate of both NCTC L929 normal mouse fibroblasts and B16/F10 mouse melanoma cells in a wide range of concentrations. However, $Ce_{0,8}Gd_{0,2}O_{2-x}$ NPs significantly reduce the mitochondrial membrane potential of these cells. Additionally, it has been shown that $Ce_{0,8}Gd_{0,2}O_{2-x}$ NPs are able to effectively reduce the clonogenic activity of B16/F10 melanoma cells under proton beam irradiation. Meanwhile, proton beam irradiation remarkably reduced the clonogenic activity and MMP of melanoma cells. Hence, $Ce_{0,8}Gd_{0,2}O_{2-x}$ NPs act as a radiosensitizer in B16/F10 mouse melanoma cells under proton beam irradiation. We assume that such radiosensitizing effect of $Ce_{0,8}Gd_{0,2}O_{2-x}$ NPs is due to a decrease of the membrane mitochondrial potential. Thus, the use of $Ce_{0,8}Gd_{0,2}O_{2-x}$ NPs in combination with proton beam irradiation is a promising approach for the effective treatment of melanoma.

KEYWORDS gadolinium, cerium oxide nanoparticles, radiosensitization, proton beam irradiation

ACKNOWLEDGEMENTS This research was funded by the Ministry of Science and Higher Education of the Russian Federation (State Assignment: 075-00224-24-03).

FOR CITATION Kolmanovich D.D., Romanov M.V., Khaustov S.A., Ivanov V.K., Shemyakov A.E., Chukavin N.N., Popov A.L. Proton beam-induced radiosensitizing effect of $Ce_{0.8}Gd_{0.2}O_{2-x}$ nanoparticles against melanoma cells *in vitro*. *Nanosystems: Phys. Chem. Math.*, 2024, **15** (5), 675–682.

1. Introduction

Radiation therapy (RT) is a modern medical approach which is being used as a full-fledged treatment of tumors, as well as a palliative therapy to relieve symptoms caused by cancer. Currently, at least 40% of cancer patients receive radiation therapy [1]. One of the main issues of RT is the risk of damage to healthy tissues. The biological effectiveness of irradiation depends on several factors, including linear energy transfer (LET), total dose, fractionation and radiosensitivity of targeted cells and tissues [2]. For instance, low-LET radiation releases relatively small amount of energy, while high-LET radiation releases a lot of energy at the target sites. Despite the fact that irradiation is aimed at killing tumor cells, it inevitably damages healthy cells nearby. Currently, the most commonly used types of radiation for the needs of radiotherapy are X-rays and gamma rays (photon-based radiation). This type of radiation is characterized by low-LET values. Because of this, gamma rays and X-rays are ineffective in the treatment of radioresistant cancers, such as sarcoma, kidney carcinoma, melanoma and glioblastoma [3,4]. In addition, one of the main disadvantages of using photon radiation is the collateral irradiation of healthy tissues along the path of the photon beam, both before and after the tumor site.

The use of proton beam therapy (PBT) makes it possible to reduce the adverse effect of irradiation on healthy tissues and, as a result, decrease the risk of PBT side effects [5]. Also, it is possible to dramatically increase the radiation dose to

the tumor in PBT, while maintaining the side effect on the surrounding healthy tissues within their tolerance limits. These advantages are primarily related to the peculiarities of the physical interaction of protons with the matter: unlike photons, which irradiate everything on their path and lose their energy exponentially, hadrons (protons and also carbon ions) have a finite path length and emit most of their energy at the end of their path [6]. This distribution of hadrons energy along the path of their run is described by the Bregg peak (BP).

In addition to the use of various types of radiation, the selection of optimal irradiation positions and dose, fractionation modes, radiosensitizers of various nature can be used to increase the effectiveness of radiotherapy. Various small organic molecules, peptides, proteins, nucleic acids and other substances can act as radiosensitizers [7, 8]. Nanoparticles based on inorganic components have recently been of the greatest interest in this capacity [9]. Unlike organic preparations, they may have a number of useful properties that extend their use. For example, superparamagnetic substances are used for imaging in MRI and particles with a metal core are used in CT [10]. The radiosensitizing effect of inorganic nanoparticles is due to the generation of secondary radiation when the ionizing beam interacts with these radiosensitizers [11]. In the case of proton beam irradiation, their inelastic Coulomb interactions with nanoparticles can lead either to the formation of free electrons, or even to the destruction of the nuclei of elements in the composition of the radiosensitizer during nuclear reactions [12]. Due to the secondary radiation production, a local dose increase occurs, which makes it possible to expand the therapeutic window. As a result of this effect, it is possible to achieve either an increase in the effectiveness of therapy without changing the administered dose, or to remain at the same treatment level while reducing the administered dose. It was believed that nanoparticles containing elements with a large atomic mass value in their composition are more suitable for radiosensitization purposes, since these elements have more electrons in the outer electron shells, which can be excited by ionizing radiation and therefore emit secondary radiation. However, in a recent study [13], it has been shown that TiO_2 nanoparticles with a relatively low effective atomic number demonstrate a significant radiosensitizing effect when irradiated with photons (150 kV and 6 MV) and protons (100 MeV). This effect may be associated with the pronounced radiocatalytic activity of these nanoparticles, which leads to the formation of hydroxyl radicals. Under proton irradiation conditions, it was found that the generation of reactive oxygen species (ROS) in the presence of TiO_2 is comparable to that in the presence of WO_3 particles and higher than in the presence of HfO_2 nanoparticles. Thus, the use of nanoparticles with radiocatalytic activity in PBT is a promising approach.

Nanodisperse cerium (IV) dioxide (aka CeO_2 NPs) has recently been an object of interest to many researchers [14,15]. In recent years, it has been found that it exhibits various enzyme-like activities. In particular, it can mimic catalase, superoxide dismutase, oxidase, etc. [16] Its enzyme-like properties are due to incomplete oxidation of cerium, which makes possible the Ce^{+3}/Ce^{+4} transitions underlying various catalytic processes on the surface of cerium oxide nanoparticles. Depending on the environmental conditions, CeO_2 NPs can exhibit both prooxidant and antioxidant activity. In a low pH environment (6.9 or less), which is typical for tumors, CeO_2 NPs tends to exhibit prooxidant activity. For instance, it has been shown that the co-cultivation of various human cancer cells, such as bronchoavolar [17] and hepatocellular carcinoma [18], with CeO_2 NPs leads to an increase in the intracellular ROS generation and therefore promotes the development of oxidative stress in these cells. Additionally, it has been shown that exposing pancreatic cancer cells loaded with CeO_2 NPs to radiation leads to a more effective reduction in their clonogenic activity, compared to using radiation alone [19]. Due to its unique physicochemical features and noticeable biological activity confirmed by many studies, nanoscale cerium (IV) dioxide can be considered as a promising radiosensitizer. To endow CeO_2 NPs with additional properties, they can be doped with the other elements. Particularly, gadolinium-doped CeO_2 NPs have demonstrated the ability to contrast in MRI [20], which can be used to visualize tumors along with their therapy. In addition, the presence of gadolinium in the composition can increase radiosensitizing properties of CeO_2 NPs. Hence, gadolinium-doped CeO_2 NPs are promising for use as theranostics (substances that have both therapeutic and diagnostic properties).

In this study, we have for the first time demonstrated the potential of using dextran-stabilized $Ce_{0.8}Gd_{0.2}O_{2-x}$ nanoparticles as an effective nanoradiosensitizer in combination with proton beam irradiation for melanoma treatment.

2. Materials and methods

2.1. Synthesis and characterization of $Ce_{0.8}Gd_{0.2}O_{2-x}$ nanoparticles

$Ce_{0,8}Gd_{0,2}O_{2-x}$ NPs were synthesized by the hydrothermal method. Briefly, a solution of mixed of cerium (III) and gadolinium (III) nitrates (0.18 and 0.02 M, respectively) and dextran ($M_r \sim 6000$) was prepared, with the ($Ce(NO_3)_3{\cdot}6H_2O$+$Gd(NO_3)_3{\cdot}6H_2O$) : dextran ratio being 1 : 2 (wt). To the continuously stirred solution, 1 M aqueous ammonia was added dropwise for 3 hours, maintaining the pH at 7.5–8.0. When the pH became constant, the mixture was stirred, for additional 2 hours, then aqueous ammonia was added to reach pH 12, followed by additional stirring for 8 hours. To the colloidal solution obtained, an excess of isopropanol was added and the mixture was refluxed to form a white precipitate. This precipitate was further washed several times with hot isopropanol and dried in air at 60°C. $Ce_{0,8}Gd_{0,2}O_{2-x}$ NPs colloidal solution was prepared by dispersing the powder in the deionized water. The size and shape of $Ce_{0,8}Gd_{0,2}O_{2-x}$ NPs were determined by transmission electron microscopy (TEM) using a Leo912 AB Omega electron microscope (Carl Zeiss, Germany) equipped with an electron energy loss spectrometer (EELS) operating at an

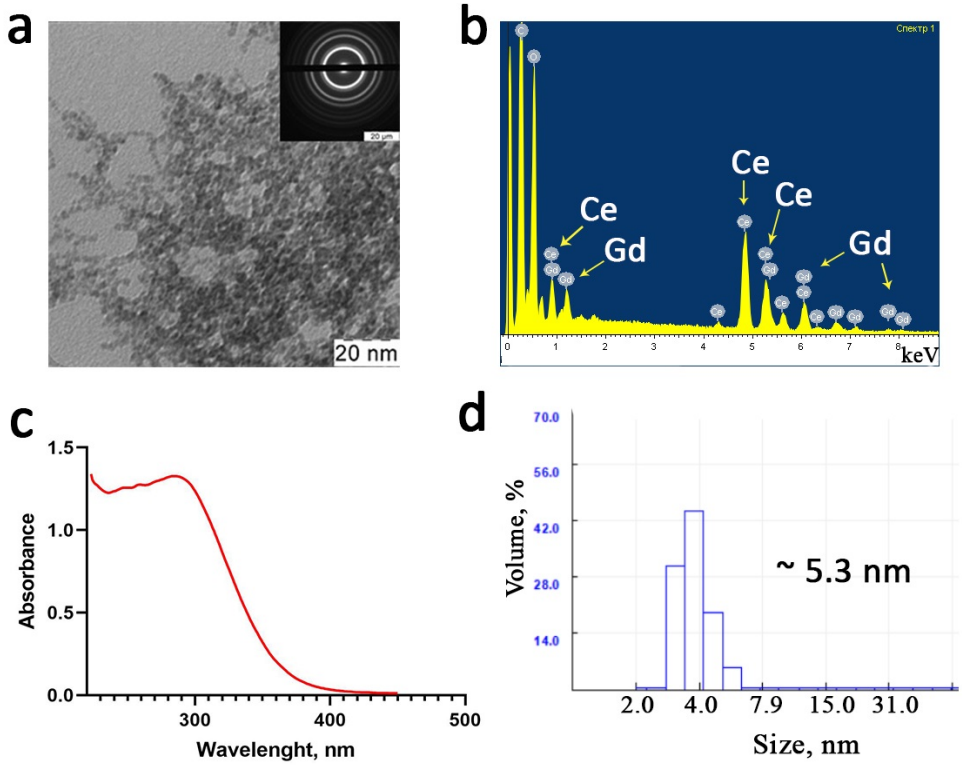

FIG. 1. TEM image with SAED pattern (inset) (a), EDX spectrum (b), UV-visible absorbance spectrum (c) and hydrodynamic diameter distribution (d) of the $Ce_{0,8}Gd_{0,2}O_{2-x}$ NPs

accelerating voltage of 100 kV. The chemical composition of $Ce_{0,8}Gd_{0,2}O_{2-x}$ nanoparticles was analyzed by energy dispersive X-ray analysis (EDX) using a NVision 40 scanning electron microscope (Carl Zeiss, Germany) equipped with an X-MAX detector (80 mm^2) (Oxford Instruments, United Kingdom) at an accelerating voltage of 20 kV. A DS-11+ spectrophotometer (DeNOVIX, USA) was used to measure absorbance of $Ce_{0,8}Gd_{0,2}O_{2-x}$ NPs water sol in the UV-visible range. The hydrodynamic diameter of $Ce_{0,8}Gd_{0,2}O_{2-x}$ nanoparticles in deionized water was measured by dynamic light scattering (DLS) using a N5 submicron particle size analyzer (Beckman Coulter, USA).

2.2. Cell culture

For cell culture experiments, NCTC L929 normal mouse fibroblasts and B16/F10 mouse melanoma cells were obtained from the cryostorage of the Theranostics and Nuclear medicine lab (ITEB RAS, Russia). The cells were cultured in DMEM/F-12 medium (1:1) (PanEco, Russia), containing 2 mM of L-glutamine, 100 U/mL of penicillin and 100 μg/mL of streptomycin (PanEco, Russia) and 10% of Fetal Bovine Serum (FBS) (HyClone, USA). Cell culture experiments were performed using Neoteric laminar boxes (Lamsystems, Russia). The cells were incubated in CO_2-incubator D180 (RWD Life Science, China) at 37°C in humidified atmosphere containing 5% CO_2. As the cells grew and reached subconfluent state, they were treated with a 0.25% trypsin-EDTA (PanEco, Russia) solution and passed into new T12, T25 or T75 cell culture flasks (SPL Life Sciences, Korea) at a ratio of 1:4.

2.3. Proton beam irradiation

T12 cell culture flask, completely filled with the culture medium, was irradiated on the "Prometheus" proton therapy complex (LPI RAS, Russia) in the Bragg peak mode at a beam energy of 160 MeV at the accelerator outlet.

2.4. Cell death analysis

Cell death analysis was performed 24, 48 and 72 hours after co-incubation with $Ce_{0,8}Gd_{0,2}O_{2-x}$ NPs or proton beam irradiation of cells. Briefly, the cell culture medium was replaced with a mixture of fluorescent dyes Hoechst 33342 (Lumiprobe, Russia), which binds to the DNA of all of the cells (Ex=350 nm, Em=460 nm), and propidium iodide (PI) (Lumiprobe, Russia), which binds to the DNA of only dead cells (Ex=535 nm, Em=615 nm), dissolved in a Hanks' Balanced Salt Solution (HBSS) (PanEco, Russia) at a concentration of 1 uM. After 15 minutes of incubation, the cells were washed twice with HBSS, and then the microphotography of the cells was carried out using ZOE fluorescent cell imager (Bio-Rad, USA). The total number of the cells and the number of dead cells were counted using the ImageJ software. After that, the percentage of dead cells was calculated.

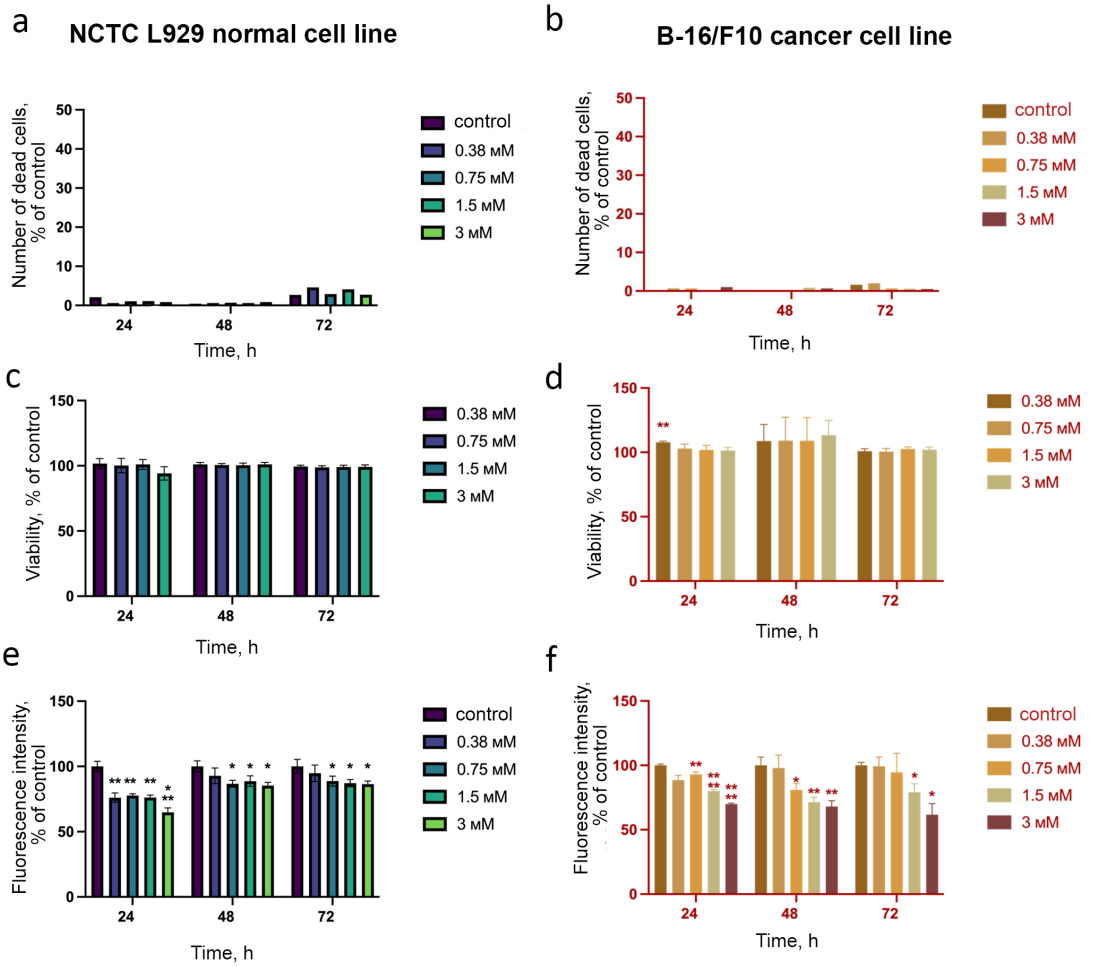

FIG. 2. Percentage of dead cells (a, b), cell viability (c, d) and mitochondrial membrane potential (e, f) of normal (NCTC L929; a, c, e) and tumor (B16/F10; b, d, f) cells after 24, 48 and 72 hours of co-incubation with $Ce_{0,8}Gd_{0,2}O_{2-x}$ NPs at concentration of 0.38–3 mM. The results are presented as a Mean ± Standard deviation (SD). The significance of the deviations between the experimental and control groups was confirmed using the Welch's t-test with the corresponding p values: $0.01<p<0.05$ (*), $0.001<p<0.01$ (**), $0.0001<p<0.001$ (***) and $p<0.0001$ (****)

2.5. Cell viability assay

Cell viability was analyzed using routine MTT-assay. Briefly, the cell culture medium was replaced with a solution of MTT (3-(4,5-dimethylthiazole-2-yl)-2,5-diphenyl-tetrazolium bromide) (PanEco, Russia) in a serum-free medium at a concentration of 0.5 mg/mL 24, 48 and 72 hours after co-incubation with $Ce_{0,8}Gd_{0,2}O_{2-x}$ NPs. MTT is being reduced by intracellular NAD(P)H-dependent oxidoreductase enzymes depending on the metabolic activity of cell and, consequently, its viability. After 3 hours of incubation, the MTT solution was replaced with DMSO (PanEco, Russia), and the plate were placed on a plate shaker for 1 minute. After that, the optical density (OD) of the resulted solutions was measured at a wavelength of 570 nm using an INNO-S plate reader (LTek, Korea). The OD values were recalculated as a percentage of the corresponding values from the control groups, the results were presented as a Mean ± Standard deviation (SD).

2.6. Analysis of mitochondrial membrane potential

Mitochondrial membrane potential (MMP) analysis was performed 24, 48 and 72 hours after co-incubation with $Ce_{0,8}Gd_{0,2}O_{2-x}$ NPs or proton beam irradiation of the cells. Briefly, the cell culture medium was replaced with a TMRE solution (tetramethylrodamine, ethyl ether) (Lumiprobe, Russia), which selectively accumulates in active mitochondria due to their transmembrane potential (Ex=550 nm, Em=575 nm), in a HBSS at a concentration of 1 uM. After 15 minutes of incubation, the cells were washed twice with HBSS, and then the microphotography of the cells was carried out using a ZOE fluorescent cell imager (Bio-Rad, USA). The fluorescence intensity of TMRE was measured using the ImageJ program and then were recalculated as a percentage of the corresponding values from the control groups, the results were presented as a Mean ± Standard deviation (SD).

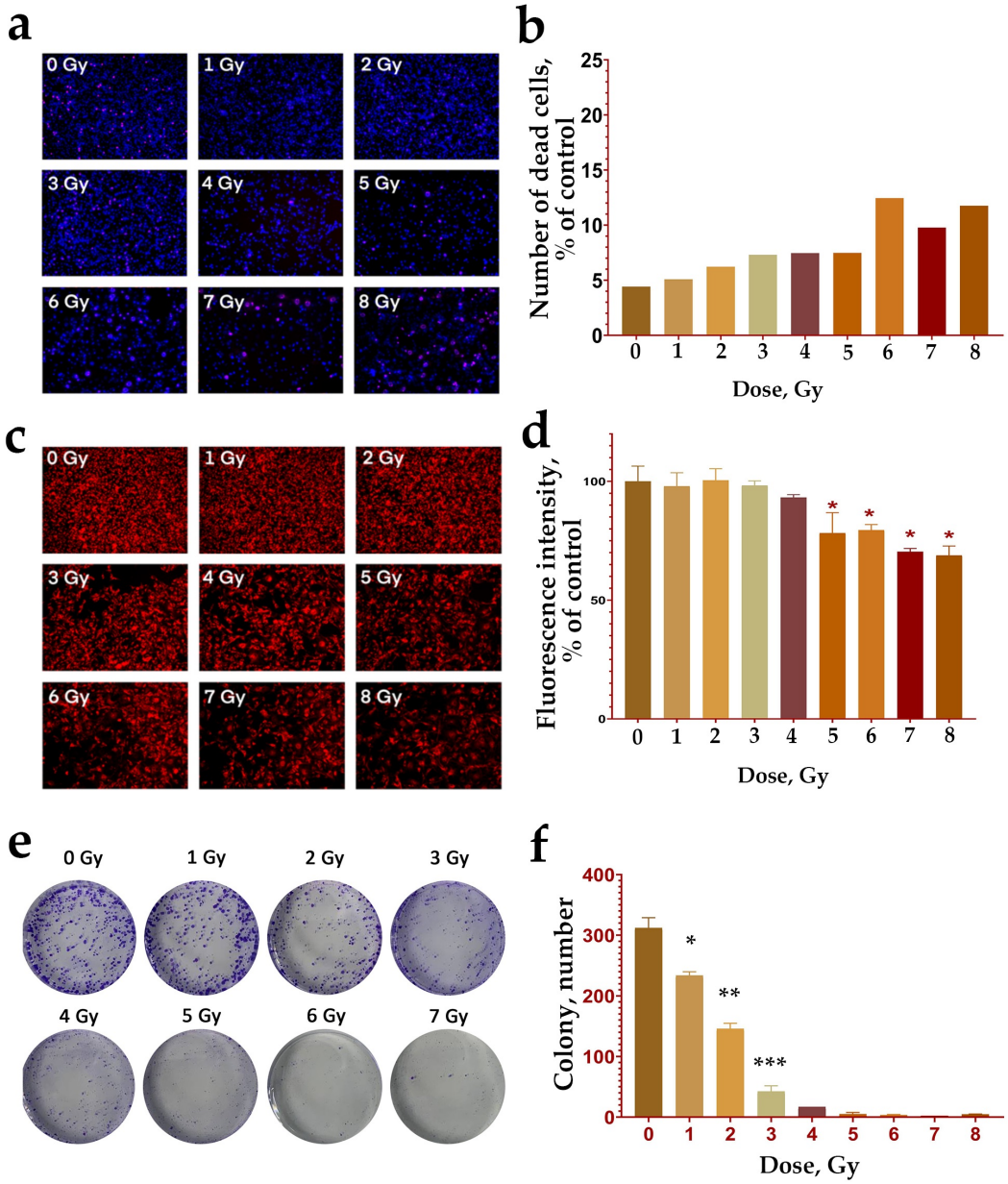

FIG. 3. The effect of proton beam irradiation on the survival (a, b), mitochondrial membrane potential (c, d) and clonogenic activity (e, f) of B16/F10 mouse melanoma cells. The results are presented as a Mean ± Standard deviation (SD). The significance of the deviations between the experimental and control groups was confirmed using the Welch's t-test with the corresponding p values: $0.01<p<0.05$ (*)

2.7. Clonogenic assay

Analysis of cell clonogenic activity was performed immediately after proton beam irradiation. The cells were seeded on a 6-well plate (SPL, Korea) with a density of 1000 cells per well. After 8 days, formed cell colonies were fixed with 4% paraformaldehyde (PanEco, Russia) and stained with 0.1% methylene blue solution (PanEco, Russia). Then cell colonies were counted manually. Colonies were considered to be cellular aggregates of 50 cells or more.

2.8. Statistical analysis

Statistical analysis was performed using a GraphPad Prism software. The significance of the deviations between the experimental and control groups was confirmed using the Welch's t-test with the corresponding p values: $0.01<p<0.05$ (*), $0.001<p<0.01$ (**), $0.0001<p<0.001$ (***) and $p<0.0001$ (****).

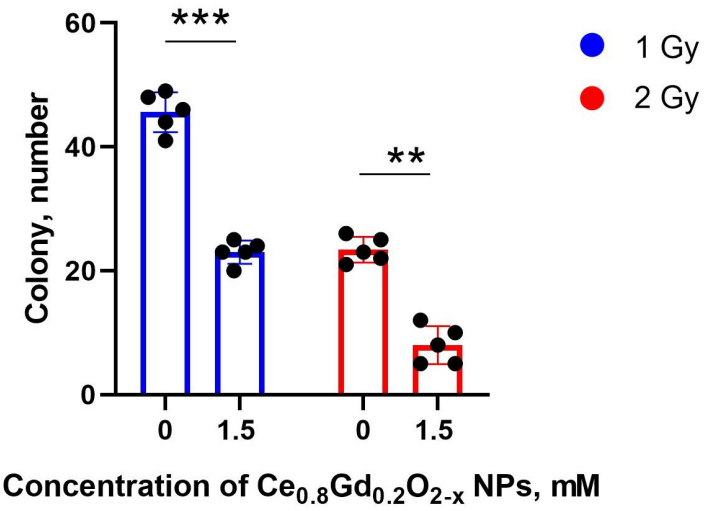

FIG. 4. $Ce_{0,8}Gd_{0,2}O_{2-x}$ NPs nanoparticles at a concentration of 1.5 mM significantly decreased the clonogenic activity of B16/F10 mouse melanoma cells under proton beam irradiation at doses of 1 and Gy. The results are presented as experimental repeats (n=5) with Mean ± Standard deviation (SD). The significance of the deviations between the experimental and control groups was confirmed using the Welch's t-test with the corresponding p values: $0.001<p<0.01$ (**) and $0.0001<p<0.001$ (***)

3. Results

The synthesized $Ce_{0.8}Gd_{0.2}O_{2-x}$ NPs colloidal solution had no eye-visible opalescence, however it demonstrated an obvious Tyndall effect. According to the transmission electron microscopy data, $Ce_{0.8}Gd_{0.2}O_{2-x}$ NPs have a spherical shape and an ultrasmall size (less than 5 nm) (Figure 1a). Energy dispersive X-ray spectroscopy has shown that the chemical composition of the sample corresponds well to the chemical formula $Ce_{0.8}Gd_{0.2}O_{2-x}$ NPs (Fig. 1b). UV spectrum analysis (Fig. 1c) confirms the characteristic peak of Ce^{4+}. The mean hydrodynamic diameter of $Ce_{0.8}Gd_{0.2}O_{2-x}$ NPs in deionized water is approximately 5.3±3.1 nm (Fig. 1d).

Next, we conducted a comprehensive analysis of the cytotoxicity of $Ce_{0,8}Gd_{0,2}O_{2-x}$ NPs on both normal and tumor cells (Fig. 2). It has been found that $Ce_{0,8}Gd_{0,2}O_{2-x}$ NPs do not promote the death of both NCTC L929 and B16/F10 cells up to a concentration of 3 mM after 72 hours of co-incubation (Fig. 2a,b). It should be noted that the percentage of dead cells did not exceed the value of 5% even at a nanoparticle concentration of 3 mM after 72 hours of incubation. Furthermore, there was no significant decrease in the viability of both normal and tumor cells even at a $Ce_{0,8}Gd_{0,2}O_{2-x}$ NPs concentration of 3 mM after 72 hours of co-incubation (Fig. 2c,d). However, $Ce_{0,8}Gd_{0,2}O_{2-x}$ NPs significantly reduced the MMP of NCTC L929 cells at all of the studied concentrations after 24, 48 and 72 hours of co-incubation (Fig. 2e). Interestingly, there was also a notable MMP decrease in B16/F10 but only at high concentrations of $Ce_{0,8}Gd_{0,2}O_{2-x}$ NPs (0.75-3 mM) after 24, 48 and 72 hours of co-incubation. It is worth noting that $Ce_{0,8}Gd_{0,2}O_{2-x}$ NPs at concentrations of 1.5 mM and 3 mM caused a significant decrease in MMP of melanoma cells (by 30–40%), which was not observed in normal fibroblasts (Fig. 2f).

A comprehensive analysis was further conducted of the effect of proton beam irradiation on the viability parameters of mouse melanoma cells (Fig. 3). This analysis included the determination of the survival rate, MMP and clonogenic activity of B16/F10 cells after proton beam irradiation in the Bragg peak mode in a wide range of doses, ranging from 1 to 8 Gy. A dose-dependent increase in the percentage of dead cells was revealed 72 hours after irradiation at doses of 2 Gy and higher (Fig. 3a,b). It is also worth noting that an increase in the irradiation dose results in an obvious decrease in the overall number of cells seen in micrographs. This phenomenon can be explained by reduced cell proliferation and adhesion after irradiation. Meanwhile, high irradiation doses (6–8 Gy) caused the death of slightly less than 20% of the cells. It has also been demonstrated that irradiation at doses from 1 to 4 Gy did not cause a significant decrease in the MMP of B16/F10 cells (Fig. 3c,d). Nevertheless, irradiation at higher doses (from 5 to 8 Gy) significantly reduced the value of MMP by 25–35% relative to the control. In addition, the clonogenic activity of melanoma cells decreased linearly with an increase in the dose of irradiation (Fig. 3e,f). Starting with a dose of 5 Gy, no colony formation was observed, which indicates a 100% inhibitory effect of proton beam irradiation on B16/F10 cells.

It has also been shown that $Ce_{0,8}Gd_{0,2}O_{2-x}$ NPs at a concentration of 1.5 mM significantly decreased the number of B16/F10 colonies after proton beam irradiation (Fig. 4). It is worth noting that for this concentration of $Ce_{0,8}Gd_{0,2}O_{2-x}$ NPs, we did not observe a reduction in cell viability and survival, but instead observed a decrease in MMP (Fig. 2). Meanwhile, proton beam irradiation at doses of 1 and 2 Gy significantly reduced the clonogenic activity of mouse melanoma cells, and at doses of 5 Gy or above it dramatically declined the MMP of these cells. Therefore, $Ce_{0,8}Gd_{0,2}O_{2-x}$ NPs act

as a radiosensitizer in B16/F10 mouse melanoma cells under proton beam irradiation. We hypothesize that this radiosensitizing effect of $Ce_{0,8}Gd_{0,2}O_{2-x}$ NPs is due to the hypopolarization of mitochondrial membranes, which can be caused in turn by enzyme-like activity of these nanoparticles, and this activity can also be enhanced by proton beam irradiation. Thus, $Ce_{0,8}Gd_{0,2}O_{2-x}$ NPs make it possible to use a lower dose of proton beam irradiation to kill melanoma cells.

4. Discussion

The radioresistance of tumors and the occurrence of side effects due to irradiation of healthy tissues are still urgent problems in the radiotherapy of tumors. The use of hadron therapy instead of classical photon therapy makes it possible to reduce the dose load on healthy tissues, while the use of radiosensitizers significantly increases the therapeutic effect of irradiation, thereby enhancing the effectiveness of treatment. Furthermore, the use of inorganic nanoparticles as radiosensitizers is a promising area of research and development, since such nanomaterials exhibit a wide variety of features inaccessible to organic substances, while their production is neither expensive nor time-consuming. Nanoscale cerium (IV) dioxide has a great potential for use in radiotherapy. Long-term studies on this substance have demonstrated its ability to exhibit selective cytotoxicity against tumor cells as well as to enhance the therapeutic effect of radiotherapy. Our study was aimed at expanding our understanding of the potential of using $Ce_{0,8}Gd_{0,2}O_{2-x}$ NPs in proton therapy of melanoma. We have demonstrated that $Ce_{0,8}Gd_{0,2}O_{2-x}$ NPs are able to dramatically reduce the clonogenic activity of melanoma cells under proton beam irradiation. Also, $Ce_{0,8}Gd_{0,2}O_{2-x}$ NPs promoted a decrease in MMP of these cells. Meanwhile, proton beam irradiation also reduced the clonogenic activity and MMP of melanoma cells. Hence, $Ce_{0,8}Gd_{0,2}O_{2-x}$ NPs act as a radiosensitizer in B16/F10 mouse melanoma cells under proton beam irradiation. We assume that such radiosensitizing effect of $Ce_{0,8}Gd_{0,2}O_{2-x}$ NPs is due to a decrease of the membrane mitochondrial potential, which can be due to enzyme-like activity of these nanoparticles. Moreover, their catalytic activity can also be enhanced by proton beam irradiation. Thus, the use of $Ce_{0,8}Gd_{0,2}O_{2-x}$ NPs in combination with proton beam irradiation is a promising approach for the effective treatment of melanoma. Since this work was conducted only on 2D cell cultures *in vitro*, it seems actual to study the radiosensitizing and MRI-labeling properties of $Ce_{0,8}Gd_{0,2}O_{2-x}$ NPs on both 3D tumor spheroids *in vitro* and mouse tumor model *in vivo* to reveal its theranostic nature.

References

[1] Ringborg U., Bergqvist D., Brorsson B., Cavallin-ståhl E., Ceberg J., Einhorn N., Frödin J., Järhult J., Lamnevik G., Lindholm C., Littbrand B., Norlund A., Nylén U., Rosén M., Svensson H., Möller T. The Swedish Council on Technology Assessment in Health Care (SBU) Systematic Overview of Radiotherapy for Cancer Including a Prospective Survey of Radiotherapy Practice in Sweden 2001–Summary and Conclusions. *Acta Oncol.* **2003**.

[2] Baskar R., Lee K.A., Yeo R., Yeoh K.-W. Cancer and Radiation Therapy: Current Advances and Future Directions. *Int. J. Med. Sci.*, 2012, **9**, P. 193–199.

[3] Yalamarty S.S.K., Filipczak N., Li X., Subhan M.A., Parveen F., Ataide J.A., Rajmalani B.A., Torchilin V.P. Mechanisms of Resistance and Current Treatment Options for Glioblastoma Multiforme (GBM). *Cancers*, 2023, **15**, P. 2116.

[4] Gregucci F., Beal K., Knisely J.P.S., Pagnini P., Fiorentino A., Bonzano E., Vanpouille-Box C.I., Cisse B., Pannullo S.C., Stieg P.E., et al. Biological Insights and Radiation–Immuno–Oncology Developments in Primary and Secondary Brain Tumors. *Cancers*, 2024, **16**, P. 2047.

[5] Mohan R. A Review of Proton Therapy – Current Status and Future Directions. *Precis. Radiat. Oncol.*, 2022, **6**, P. 164–176.

[6] Chen, Z.; Dominello, M.M.; Joiner, M.C.; Burmeister, J.W. Proton versus Photon Radiation Therapy: A Clinical Review. *Front. Oncol.* **2023**, **13**.

[7] Wang, H.; Mu, X.; He, H.; Zhang, X.-D. Cancer Radiosensitizers. *Trends Pharmacol. Sci.* **2018**, **39**, P. 24–48.

[8] Gong, L.; Zhang, Y.; Liu, C.; Zhang, M.; Han, S.; Application of Radiosensitizers in Cancer Radiotherapy. *Int J Nanomedicine.* **2021**, 16, P. 1083–1102. Erratum in: *Int J Nanomedicine.*, 2021, **16**, P. 8139–8140.

[9] Varzandeh M., Sabouri L., Mansouri V., Gharibshahian M., Beheshtizadeh N., Hamblin M.R., Rezaei N. Application of Nano-Radiosensitizers in Combination Cancer Therapy. *Bioeng. Transl. Med.* **2023**, **8**, P. e10498.

[10] Laurent S., Mahmoudi M. Superparamagnetic Iron Oxide Nanoparticles: Promises for Diagnosis and Treatment of Cancer. *Int. J. Mol. Epidemiol. Genet.*, **2011**, **2**, P. 367–390.

[11] Zavestovskaya I.N., Filimonova M.V., Popov A.L., Zelepukin I.V., Shemyakov A.E., Tikhonowski G.V., Savinov M., Filimonov A.S., Shitova A.A., Soldatova O.V., et al. Bismuth Nanoparticles-Enhanced Proton Therapy: Concept and Biological Assessment. *Mater. Today Nano*, 2024, **27**, P. 100508.

[12] Newhauser W.D., Zhang R. The Physics of Proton Therapy. *Phys. Med. Biol.*, 2015, **60**, P. R155.

[13] Gerken L.R.H., Gogos A., Starsich F.H.L., David H., Gerdes M.E., Schiefer H., Psoroulas S., Meer D., Plasswilm L., Weber D.C., et al. Catalytic Activity Imperative for Nanoparticle Dose Enhancement in Photon and Proton Therapy. *Nat. Commun.*, 2022, **13**, P. 3248.

[14] Wei H., Wang E. Nanomaterials with Enzyme-like Characteristics (Nanozymes): Next-Generation Artificial Enzymes. *Chem. Soc. Rev.*, 2013, **42**, P. 6060–6093.

[15] Wu J., Wang X., Wang Q., Lou Z., Li S., Zhu Y., Qin L., Wei H. Nanomaterials with Enzyme-like Characteristics (Nanozymes): Next-Generation Artificial Enzymes (II). *Chem. Soc. Rev.*, 2019, **48**, P. 1004–1076.

[16] Popov A.L., Shcherbakov A.B., Zholobak N.M., Baranchikov A.E., Ivanov V.K. Cerium Dioxide Nanoparticles as Third-Generation Enzymes (Nanozymes). *Nanosyst. Phys. Chem. Math.*, **2017**, P. 760–781.

[17] Lin W., Huang Y., Zhou X.-D., Ma Y. Toxicity of Cerium Oxide Nanoparticles in Human Lung Cancer Cells. *Int. J. Toxicol.*, 2006, **25**, P. 451–457.

[18] De Marzi L., Monaco A., De Lapuente J., Ramos D., Borras M., Di Gioacchino M., Santucci S., Poma A. Cytotoxicity and Genotoxicity of Ceria Nanoparticles on Different Cell Lines in Vitro. *Int. J. Mol. Sci.*, 2013, **14**, P. 3065–3077.

[19] Wason M.S., Colon J., Das S., Seal S., Turkson J., Zhao J., Baker C.H. Sensitization of Pancreatic Cancer Cells to Radiation by Cerium Oxide Nanoparticle-Induced ROS Production. *Nanomedicine Nanotechnol. Biol. Med.*, 2013, **9**, P. 558–569.

[20] Kolmanovich D.D., Chukavin N.N., Savintseva I.V., Mysina E.A., Popova N.R., Baranchikov A.E., Sozarukova M.M., Ivanov V.K., Popov A.L. Hybrid Polyelectrolyte Capsules Loaded with Gadolinium-Doped Cerium Oxide Nanoparticles as a Biocompatible MRI Agent for Theranostic Applications. *Polymers*, 2023, **15**, P. 3840.

Submitted 26 July 2024; accepted 14 October 2024

Information about the authors:

Danil D. Kolmanovich – Institute of Theoretical and Experimental Biophysics of the Russian Academy of Sciences, Pushchino, Russia; ORCID 0000-0003-3391-7889; kdd100996@mail.ru

Mikhail V. Romanov – Institute of Molecular Theranostics, Sechenov First Moscow State Medical University, Moscow, Russia; Lopukhin Federal Research and Clinical Center of Physical-Chemical Medicine of Federal Medical Biological Agency, Moscow, Russia; ORCID 0009-0005-8700-1536; romanov.mikhail@phystech.edu

Sergey A. Khaustov – Scientific and Educational Center, State University of Education, Moscow, Russia; ORCID 0000-0001-9286-3644; sergeykhaustov@gmail.com

Vladimir K. Ivanov – Kurnakov Institute of General and Inorganic Chemistry of the Russian Academy of Sciences, Moscow, Russia; ORCID 0000-0003-2343-2140; van@igic.ras.ru

Alexander E. Shemyakov – Institute of Theoretical and Experimental Biophysics of the Russian Academy of Sciences, Pushchino, Russia; Lebedev Physical Institute of the Russian Academy of Sciences, Moscow, Russia; ORCID 0000-0003-1175-6703; alshemyakov@yandex.ru

Nikita N. Chukavin – Institute of Theoretical and Experimental Biophysics of the Russian Academy of Sciences, Pushchino, Russia; Scientific and Educational Center, State University of Education, Moscow, Russia; ORCID 0000-0001-8431-4485; chukavinnik@gmail.com

Anton L. Popov – Institute of Theoretical and Experimental Biophysics of the Russian Academy of Sciences, Pushchino, Russia; Scientific and Educational Center, State University of Education, Moscow, Russia; ORCID 0000-0003-2643-4846; antonpopovleonid@gmail.com

Conflict of interest: the authors declare no conflict of interest.